A Simplified Approach Based on Cellular Automata for Describing Direct Reduced Iron Production in Different Reducing Conditions

Carlo Mapelli,* Gianluca Dall'Osto, Davide Mombelli, Matteo Carmelo Romano, Roberto Scaccabarozzi, and Maurizio Spinelli

A quick computation approach based on cellular automata is developed and implemented to describe the reduction of iron ore pellets by a mixture of reducing agents featured by different H_2/CO ratios. The evolution of oxygen concentration inside the pellet is followed from the beginning to the end of contact between reducing agent and pellet. The variation of thermal state of pellets and gas mixture is computed based on their initial temperature, considering the heat involved and the convective heat exchange between pellet and gas mixture. The use of cellular automata and finite-difference method to solve the diffusion equation point out the absence of any diffusion coefficient value, allowing to make the model fit the experimental trial, because the problem is that it is not ruled just by diffusion but also by the concentration variation of reducing agent inside the pellet due to porosity increasing during reduction. The updating of the reducing agents concentration implies a sharp decrease of oxygen concentration that the cellular automata model considers. The developed model is able to provide the in-line control of reduction process and could be used to adjust the chemical concentration and temperature of injected reducing agents.

1. Introduction

The direct reduction (DR) of iron ore by either natural gas or hydrogen is receiving increasing attention as a reliable and feasible alternative to the reduction process performed by blast furnace through the exploitation of coke and coal. The DR route implies a significant decrease of greenhouse gas emission (i.e., CO_2) and even the achievement of a zero-emission scenario when biomethane or hydrogen are used as a reducing agent.[1–6]

Simulation models that can provide fast computation of the reduction process and of the change of atmosphere in reducing reactors are needed for implementing a reliable automation of process that can ensure the desired process efficiency. Alamsari et al. proposed a complex model based on the precise solution of differential equations involving heat and mass exchange and they compared their results to industrial data provided by a Midrex plant.[7] On the other hand, in such a model, several concerns affect the computation of heat exchange and so the reliability of obtained results. On the contrary, de Castro et al. designed and performed a model based on multiphase theory that describes the thermal state and diffusion phenomena of the whole DR reactor.[8] However, the simulation focused mainly on gas flow characteristic and temperature distribution, without a direct comparison with actual plant data nor expected metallization. Although these models point out interesting results, the long computational times required hinder their use for the in-line control of the process. Indeed, a simulation model for in-line control of the process must combine reliability and a computational process that is quick enough to allow feedback in order to change process parameters in time.

A simulation approach based on cellular automata accomplishes reliability and a computational time consistent with an in-line control. Cellular automata can simulate the behavior of complex systems through the interaction of the nodes where each node is cellular automaton. Cellular automata compose of a system of objects that vary their states over time on the basis of the initial conditions and of the rules that impose the interactions among the nodes, because the state (value) of each cellular automaton is determined by the state of its neighborhood.

A set of simple rules can produce a pattern assigning a specific value to each node of the grid. The cellular automata is a powerful tool for simulating the transport of matter.[9] Cellular automata allow incorporating naturally the algorithms that compute

C. Mapelli, G. Dall'Osto, D. Mombelli
Dipartimento di Meccanica
Politecnico di Milano
Via La Masa 1, 20156 Milano, Italy
E-mail: carlo.mapelli@polimi.it

M. C. Romano
Dipartimento di Energia
Politecnico di Milano
Via Lambruschini, 4, 20156 Milano, Italy

R. Scaccabarozzi, M. Spinelli
Laboratorio per l'Energia e l'Ambiente Piacenza (LEAP) s.c.a r.l.
Via Nino Bixio, 27C, 29121 Piacenza, Italy

The ORCID identification number(s) for the author(s) of this article can be found under https://doi.org/10.1002/srin.202300411.

solutions of different problems. In the case of the reduction of iron ores, the solutions of matter and thermal diffusion have been implemented, because the synchronized cellular automata are more suitable in terms of calculating the speed if compared with other computational techniques.[10] A significant advantage of models built by cellular automata is their modularity, where each module is focused on the solution of specific issues (e.g., diffusion, stirring, swelling of a solid structure) and the capability of the modules to exchange their results.[11] This makes the computational system simpler than the solution of the overall differential equation-based models since it decreases the effort of model design and coding.[12,13] Moreover, the models based on cellular automata are intrinsically coarse grained and so internal degrees of freedom and complex chemical–physical interactions are left out. Thanks to these features, cellular automata models are also robust for formulations based on large spatial and timescales ranging from nanometers to millimeters and nanoseconds to seconds and have been successfully applied to mass transfer problems, diffusion problems, chemical etching corrosion, and simulation of gas–solid reactions in complex porous media.[14–24]

Most of the models based on cellular automata run in the asynchronous modality, which means that the computation of variables is applied one after another to each cell composing the grid.

The applications of this approach in the steel- and iron-related fields have focused almost exclusively on modeling the solidification structure in continuous casting or cooling,[25-29] the recrystallization structure after heat treatment or hot working,[30-36] and corrosion.[37,38] To date and to the authors' knowledge, only two studies, both conducted by He et al.,[39,40] have focused on the reduction of iron oxides by hydrogen alone. On the contrary, cellular automata models describing direct reduced iron (DRI) production in shaft reactors are still lacking. Although, it is well established that the reduction of iron ore pellets is positively affected by an increase of H_2 share in the reduction gas mixture as well as an increase in temperature and partial pressure, the impossibility of in situ monitoring of the actual level of metallization and porosity, and the need for costly and time-consuming campaigns to optimize process parameters in the event of their modification; the use of an accurate, low-computational-load model would provide DRI producers with an essential tool for improving plant productivity and quality.[41]

Consequently, the simulation model that has been built and presented in this work describes the reduction of a spherical pellet of iron oxide from the charging section of the reactor down to its bottom (end of reduction zone of shaft furnace), and it is based on the computation of removal of oxygen contained in iron ore as a function of: 1) diffusion of hydrogen (H_2) and carbon monoxide (CO) in the iron ore pellet and 2) thermal variation of pellet and of injected reducing gas mixtures.

The results have been compared to data made available by Midrex and to that of several experimental trials reported in literature.[2,42–44] The comparison has pointed out good agreement between the results from the proposed cellular automata model and the experimental value even when the reducing mixture has been changed through a variation of H_2 and CO ratio.

2. Model

The kinetic model describing the DR of iron ores has been developed on the basis of a cellular automata approach describing the removal of oxygen through a formalism based on the diffusion of oxygen that is ruled by diffusivity and reaction rate of H_2 and CO.

The relation has been solved in the spherical coordinate, because the pellets resemble such a shape. The removal of oxygen can be described by Equation (1).[45]

$$\frac{\partial X_O}{\partial t} = D \frac{1}{r^2} \frac{d}{dr}\left(r^2 \frac{dX_O}{dr}\right) \tag{1}$$

where X_O is the concentration of oxygen, t is time, D is the effective diffusivity and reaction rate coefficient, and r is the radius of sphere. Specifically, D is the most common macroscopic characteristic of a diffusion transfer equation and it is defined as a factor of proportionality in the Fick's law by which the mass of a chemical species. dX is diffusing in time dt through the surface normal to the diffusion direction and it is proportional to the concentration gradient of this chemical species. In this model, D is an explicit parameter and is determined on the basis of diffusivity coefficients associated with CO and H_2 and takes into account also the reaction rate for each reducing reaction that imposes the removal of oxygen. The diffusivity for the two reducing chemical species is reported in Equation (2) and (3), respectively. The binary diffusion coefficient (D) was calculated by applying Darken's relation (Equation (4)).[46]

$$D_{CO} = 9^{-10} \exp\left(-\frac{216}{8.31 \times T}\right) \tag{2}$$

$$D_{H_2} = 4 \times 10^{-9} \exp\left(-\frac{216}{8.31 \times T}\right) \tag{3}$$

$$D = X_{H_2}(t) \times D_{H_2} + X_{CO}(t) \times D_{CO} \tag{4}$$

where $X_{H_2}(t)$ is the concentration of H_2 in the atmosphere at time t, $X_{CO}(t)$ is the concentration of CO in the atmosphere at time t, and T is the temperature expressed in degree Kelvin.

In this study, the cellular automata technique has been applied to the study of iron oxide reduction by hydrogen and carbon monoxide to simulate the reduction kinetics inside the shaft furnace. The reducing reaction and the associated enthalpy variation has been considered and reported in **Table 1**.[47]

The supply of reducing agents rules the removal of the oxygen that reacts with them. Based on the removed oxygen atoms, the

Table 1. Considered reducing reactions and associated enthalpies.

Reducing reactions	Enthalpies [kJ]
$3Fe_2O_3 + CO \rightarrow 2Fe_3O_4 + CO_2$	$-0.0381 * T + 19.467$
$Fe_3O_4 + CO \rightarrow 3FeO + CO_2$	$0.0024 * T + 0.2493$
$FeO + CO \rightarrow Fe + CO_2$	$0.2325 * T - 195.43$
$3Fe_2O_3 + H_2 \rightarrow 2Fe_3O_4 + H_2O$	$-0.0284 * T - 22.305$
$Fe_3O_4 + H_2 \rightarrow 3FeO + H_2O$	$-0.0073 * T + 42.022$
$FeO + H_2 \rightarrow Fe + H_2O$	$0.2228 * T - 153.66$

ADVANCED
SCIENCE NEWS

www.advancedsciencenews.com

steel
research
international

www.steel-research.de

concentrations of CO and H_2O are computed and rearranged according to the water shift gas reaction (Equation (5)).

$$CO + H_2O \rightarrow CO_2 + H_2 \qquad (5)$$

The development of the right side of Equation (1) implies

$$\frac{\partial X_O}{\partial t} = D\frac{1}{r^2}\left(r^2\frac{d^2 X_O}{dr^2} + 2r\frac{dX_O}{dr}\right) \qquad (6)$$

The solution of Equation (6) by finite-different method according to the grid in **Figure 1** implies that at current time t_1, the oxygen concentration inside the pellet at coordinate r can be determined by Equation (7).

$$X_O(r,t_1) = X_O(r,t_0)$$
$$+ D\frac{1}{r^2}\left(r^2 \frac{\frac{X_O(r_2,t_0)-X_O(r,t_0)}{r_2-r} - \frac{X_O(r,t_0)-X_O(r_1,t_0)}{r-r_1}}{\frac{r_2-r}{2}+\frac{r-r_1}{2}} \right.$$
$$\left. \times 2r\frac{X_O(r_2,t_0)-X_O(r_1,t_0)}{r_2-r_1}\right)(t_1-t_0) \qquad (7)$$

The initial condition for X_O is 0.606, that is, the theoretical oxygen concentration of hematite (Fe_2O_3), but it may be changed as a function of another oxygen concentration of raw materials.

In order to determine the chemical compositions of the atmosphere surrounding the pellets for each generic time step, the removal of oxygen mass has been computed and then the chemical composition of the pellet and of the surrounding atmosphere have been updated.

The formalism based just on a diffusion process cannot find a solution-fitting experimental data. The reduction process imposing the removal of oxygen makes the reduced volume more permeable to the transport of the reducing gas and so $X_O(r_2,t_0)$ is updated as a function of oxygen that has been already removed. Actually, the channel formation inside pellet increases as the removal of oxygen goes on. This statement points out the importance of the behavior process of pellets during reduction, because low concentrations of SiO_2, Al_2O_3, and CaO avoid formation of nonpermeable phases that can slower the diffusion of reducing phases.[48]

In contrast, channel formation positively affects the transport of reducing gases within the pellets, in agreement with the design of this cellular automata model that depicts an inverse relationship between porosity and oxygen concentration (**Figure 2**).[41]
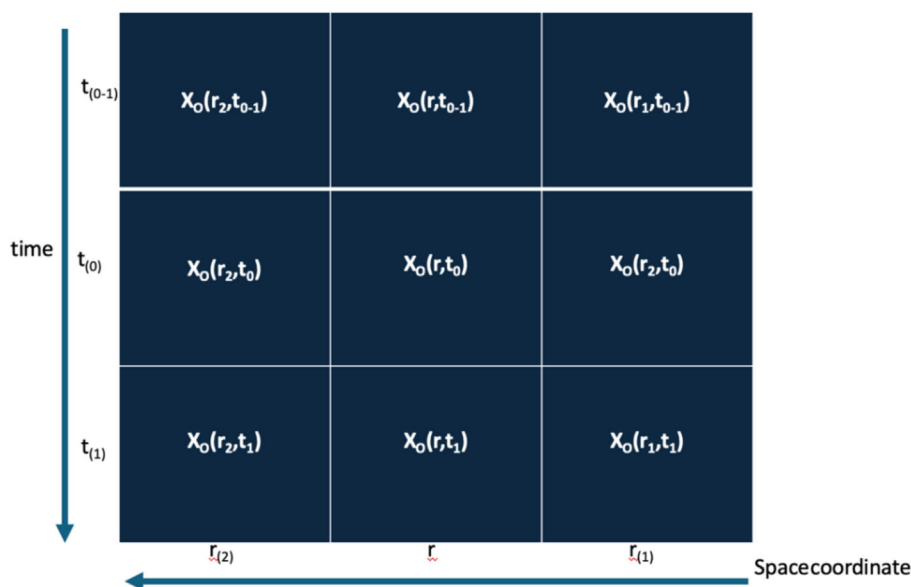
Figure 1. Grid for the solution of finite different approach.
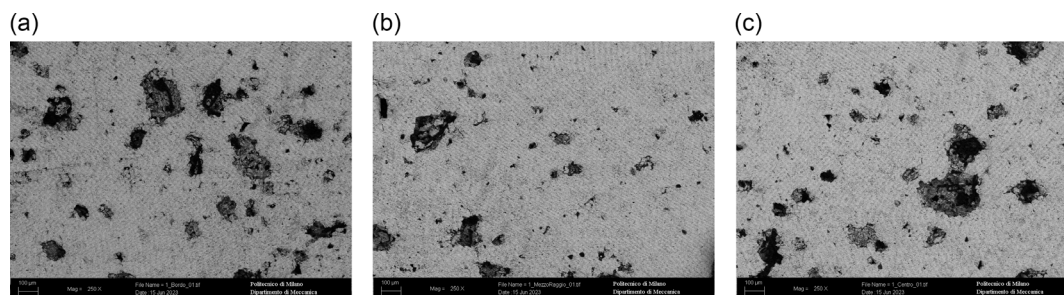
Figure 2. Examples of porosities opened on a DRI particle observed in a pellet 16 mm diameter reduced at 950 °C in an atmosphere composed 33.5% CO and 66.5% H_2 in 20 min at a) surface, b) centerline, and c) core.

2300411 (3 of 8)

**ADVANCED
SCIENCE NEWS**
www.advancedsciencenews.com

**steel research
international**
www.steel-research.de

A relation for this forced decrease of oxygen concentration in each cell on the basis of oxygen removal (caused by fast transport of reducing agents) has been tuned on the basis of experimental analysis available in literature. Specifically, Equation (2), (3), and (8) have been tuned by the application of the model to data of reaction kinetics performed by Li et al.[13] and Zuo et al.[49]

$$X_O(r_2, t_0) = \left(\frac{X_O(r_2, t_{(0-1)})}{0.606} \right) \tag{8}$$

Thus, a dynamic adjustment of the concentration of reducing elements and of the corresponding oxygen removal has been applied to take into account the pores opening in the pellet during the reduction and their effects on improving the transport of reducing agents.

The model handles also the coexistence of different oxidized phases inside the same layer as a function of oxygen concentration inside the pellets (**Table 2**).

Such an approach fits better reality than the so-called onion model where each layer is composed by just one phase as assumed by Alamsari et al.[7] This is because the volume inside the direct reduced iron (obtained from pellets) points out the coexistence of different phases as a function of oxygen concentration (**Figure 3** and **Table 3**).

The removed mass of oxygen (Δm_O) is computed step by step by Equation (9) with symbols that refer to the grid in Figure 1.

$$\Delta m_O = \frac{4}{3}\pi \left[\left(\frac{r_2 + r}{2}\right)^3 - \left(\frac{r + r_1}{2}\right)^3 \right] \frac{[X_O(r, t_0) - X_O(r, t_1)]}{0.6}$$
$$\times \rho_{pellet} \frac{1}{(\nu_0 \times 16 + \nu_{Fe} \times 55)} \nu_O \tag{9}$$

Table 2. Phases present in the pellet as a function of oxygen concentration.

Oxygen concentration (X_O)	X_i molar fraction of i-sm chemical species	
$X_O \geq 0.6$	$X_{Fe_2O_3} = 1$	
$0.57 \leq X_O < 0.6$	$X_{Fe_2O_3} = \frac{X_O - 0.57}{0.6 - 0.57}$	$X_{Fe_3O_4} = 1 - X_{Fe_2O_3}$
$0.5 \leq X_O < 0.57$	$X_{Fe_3O_4} = \frac{X_O - 0.5}{0.57 - 0.5}$	$X_{FeO} = 1 - X_{Fe_3O_4}$
$0 < X_O < 0.5$	$X_{FeO} = \frac{X_O - 0}{0.5 - 0}$	$X_{Fe} = 1 - X_{FeO}$
$X_O = 0$	$X_{Fe} = 1$	

Table 3. SEM–energy dispersive spectroscopy (EDS) spectra of micrograph in Figure 3 (wt%).

Spectra	Fe	O
A	77	23
B	100	–

where ρ_{pellet} is the density of the oxidized pellet (3200 kg m^{-3}). ν_0 and ν_{Fe} are the stoichiometric coefficients featuring the layers as a function of their composition in order to compute the correct mole fraction of oxidized species in each layer (Equation (10) and (11)).

$$\nu_{Fe} = 2 \times X_{Fe_2O_3} + 3 \times X_{Fe_3O_4} + 1 \times X_{FeO} \tag{10}$$

$$\nu_O = 3 \times X_{Fe_2O_3} + 4 \times X_{Fe_3O_4} + 1 \times X_{FeO} \tag{11}$$

Finally, based on this, the chemical variation of the atmosphere is computed. The partition of Δm_O between H_2O and CO_2 is defined as a function of H_2 and CO diffusion (Equation (12) and (13)).

$$x_{H_2O} = \frac{D_{H_2}}{D_{H_2} + D_{CO}} \tag{12}$$

$$x_{CO_2} = \frac{D_{CO}}{D_{H_2} + D_{CO}} \tag{13}$$

The partition coefficients are multiplied by the removed mass of oxygen divided by the atomic mass and multiplied for the molar mass of H_2O and CO_2 (Equation (14) and (15)).

$$\Delta m_{H_2O} = x_{H_2O} \Delta m_O \frac{2 + 16}{16} \tag{14}$$

$$\Delta m_{CO_2} = x_{CO_2} \Delta m_O \frac{12 + 32}{16} \tag{15}$$

On the basis of this computation, the variations of the concentration of H_2, CO, H_2O, and CO_2 are computed step by step and the trends featuring the atmosphere in shaft furnace evaluated.

The computation of thermal variation of pellets and of the reducing atmosphere needs an iterative procedure because, in case of counterflow between pellets and injected reducing gas, the pellet temperature is known just at the top of furnace, whereas the temperature of atmosphere is known just at the
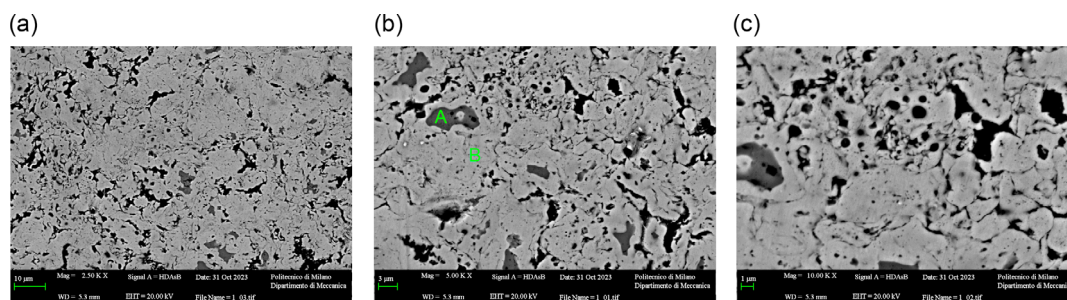
Figure 3. Scanning electron microscope-backscattered electron (SEM–BSE) micrograph at the core of a pellet (16 mm diameter) after reduction at 950 °C for 15 min, featured by coexistence of reduced iron (Fe) and residual wustite (FeO$_x$) at increasing magnification: a) 2000×, b) 5000×, and c)10 000×.

bottom and their evolution modifies the diffusivity of reducing gas inside the pellet. The thermal variations of gas and pellets for each position and time are described by Equation (16) and (17).

$$T_{t_0}^{atm} = T_{t_1}^{atm} + \frac{\Delta H_{t_1}}{m_{atm}c_{p,atm}} - h(T_{t_1}^{atm} - T_{t_1}^{pel})4\pi R^2(t_1 - t_0) \qquad (16)$$

$$T_{t_1}^{pel} = T_{t_0}^{pel} + \frac{\Delta H_{t_0}}{m_{pel}c_{p,pel}} + h(T_{t_0}^{atm} - T_{t_0}^{pel})4\pi R^2(t_1 - t_0) \qquad (17)$$

where $T_{t_0}^{atm}$ is the temperature of reducing atmosphere at time t_0, $T_{t_1}^{atm}$ is the temperature of reducing atmosphere at time t_1, $T_{t_0}^{pel}$ is the temperature of pellet at time t_0, $T_{t_1}^{pel}$ is the temperature of pellet at time t_1, ΔH_{t_1} is the enthalpy involved (developed or absorbed) in the reduction reactions at time t_1, ΔH_{t_0} is the enthalpy involved (developed or absorbed) in the reduction reactions at time t_0, h is the convective coefficient of heat exchange ($12\,W\,m^{-2}K^{-1}$), R is the radius of pellets, m_{atm} is the mass of atmosphere interacting with each pellet, m_{pel} is the mass of each pellet, t_1 is the time corresponding to the lower cell in the solution grid, and t_0 is the time corresponding to the upper cell in the solution grid. Finally, index t_1 and t_0 for the two expressions are inverted because the gas of reducing atmosphere arises from the

bottom and the pellets go down from the top of the furnace to the bottom.

In each iteration, the reducing process is computed as a first step and the thermal process as a second step; then the new temperature field is applied to determine the diffusion ruling the reducing process and after that a new thermal field is computed again and so on. After just seven iterations, the system is stable from a computational point of view, because the percentage difference between the parent step and the new one is lower than 0.05%.
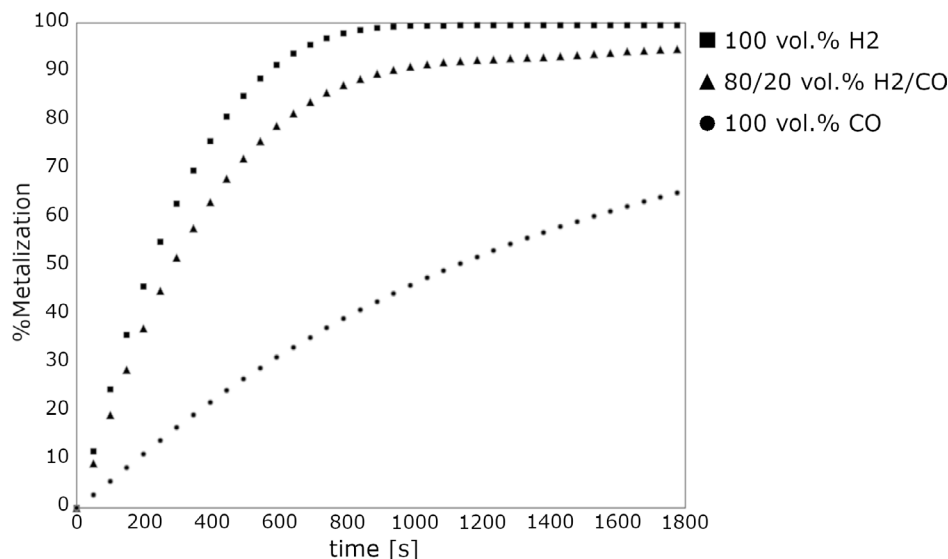
3. Validation and Comparison with Experimental Data

The model based on cellular automata points out a transformation kinetics typical of nucleation and growth of a metallic phase (**Figure 4**). The trends are similar to the pattern pointed out by a Johnson–Mehl–Avrami–Kohnogorov (JMAK) model especially on the surface layers of pellets.[50]

Although molar oxygen concentration could seem high, the computed overall oxygen amount decreases significantly because the volume at the core of pellet is much lesser than on the surface layer. Thus, a comparison between measured metallization in
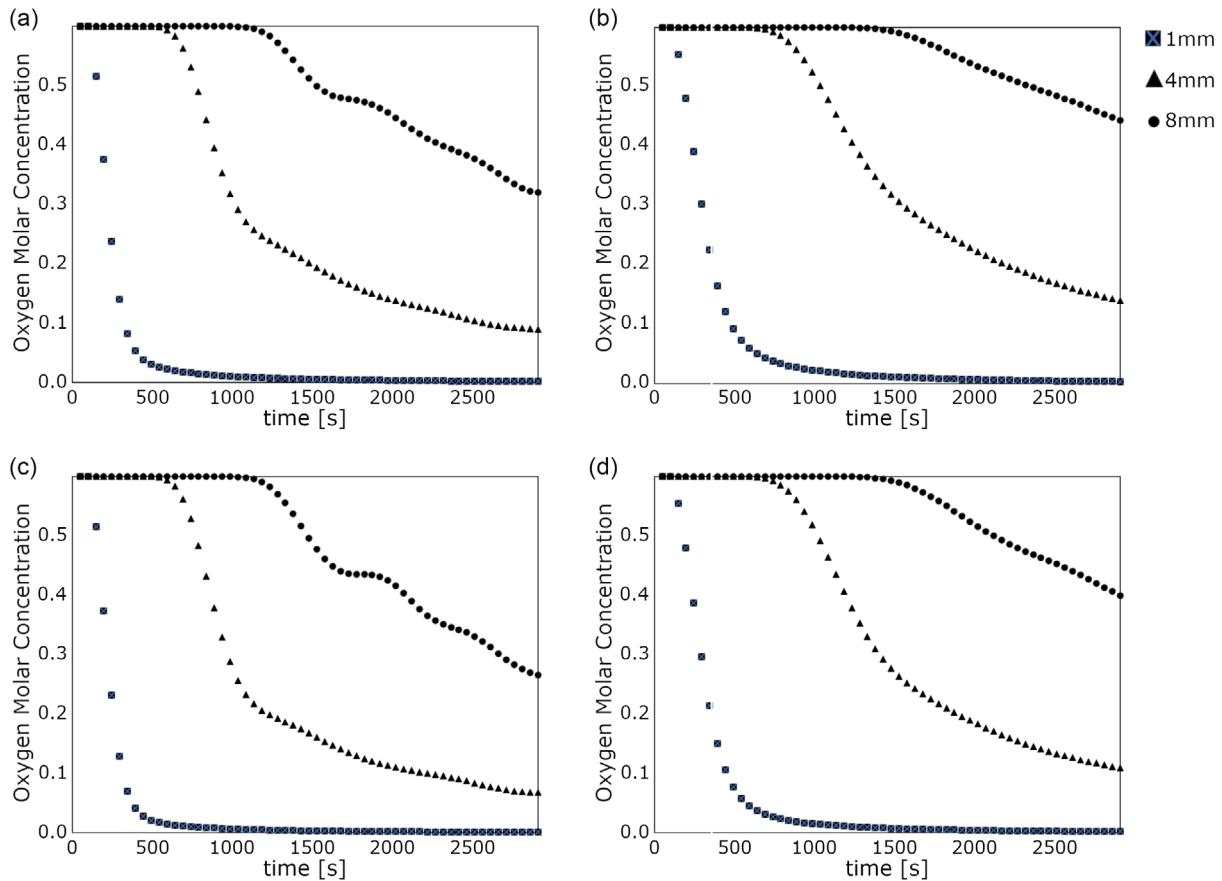
Figure 4. Oxygen variation obtained at different depths from the pellet surface (1 mm, 4 mm, and core (8 mm)) reduced at a) 850 °C in 100 vol% H_2 atmosphere, b) 850 °C in 33/66 vol% CO/H_2 atmosphere, c) 950 °C in 100 vol% H_2 atmosphere, and d) 950 °C in 33/66 vol% CO/H_2 atmosphere.

ADVANCED
SCIENCE NEWS
www.advancedsciencenews.com

steel
research
international

www.steel-research.de

Figure 5. Trend of metallization as a function of time for a pellet featured by a diameter of 16 mm reduced in an atmosphere at 850 °C in three cases: 100 vol% H_2, 100 vol% CO, and 80/20 vol% H_2/CO.

controlled condition and the results of the model based on cellular automata has been performed.

The computed trends fit the trends obtained experimentally by Bonalde et al.[42] for metallization as a function of time in three different reducing atmospheres (**Figure 5**). In order to appreciate the compliance between the experimental values and the computed ones, they have been also compared directly (**Figure 6**).

The validation of the model for a shaft furnace condition has been performed also through a comparison with data provided by Midrex, and literature data regarding the temperature of pellets, gas, and chemical composition of atmosphere point out good matching (**Table 4** and **5**).[7,51]

The model computes the evolution of reduction, evolution of temperatures, and chemical concentration of atmosphere in 0.05 s by a 2.9 GHz Intel Core i7 quad core that makes the model

reliable and suitable for online applications. The mean squared error (MSE) and root mean square error (RMSE) for the chemical composition computed in Table 4 and 5 are 3.87 (vol%)^2 and 1.96 vol%, respectively.

Table 4. Comparison between data provided by Midrex and estimated by the model based on cellular automata.

	T [K]	CH_4	H_2	CO	H_2O	CO_2
Initial condition provided by Midrex (vol%)[7]	1203	2.9	71.86	16.5	2.34	2.26
Top gas provided by Midrex (vol%)[7]	657.5	4.4	49.70	12.1	23.4	9.0
Estimated Values of Top gas from the model based on cellular automata (vol%)	687	2.0	50.90	12.7	22.3	10.6

Table 5. Comparison between data provided by Midrex at Siderca and Gilmore plants and estimated by the model based on cellular automata.

Siderca Plant	CH_4	H_2	CO	H_2O	CO_2	%Metallization
Initial condition (vol%)[51]	4.65	52.9	34.7	5.17	2.47	Not given
Top gas (vol%)[51]	6.1	49	23.6	–	(21.3)	93.8
Estimated Values of Top gas from the model based on cellular automata (vol%)	3.74	44.5	31.4	14.12	6.29	92.8

Gilmore Plant	CH_4	H_2	CO	H_2O	CO_2	
Initial condition (vol%)[51]	8.1	52.58	29.97	4.65	4.8	Not given
Top gas (vol%)[51]	8.6	37	18.9	21.2	14.3	92.8
Estimated Values of Top gas from the model based on cellular automata (vol%)	7.03	39.27	25.76	17.35	12.23	91.6
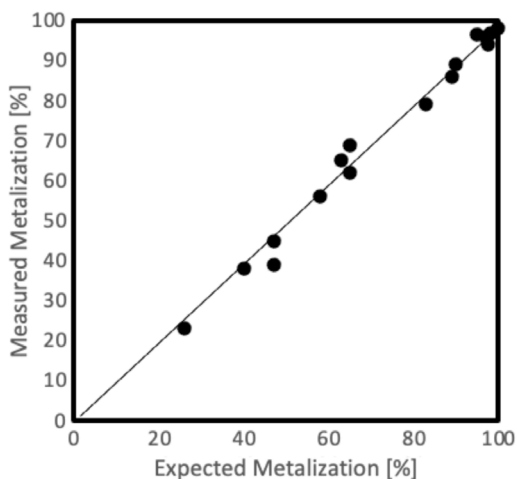
Figure 6. Comparison between the results obtained by Bonalde et al. and the reduction kinetics forecast by the model.[42]

2300411 (6 of 8)

4. Conclusion

1) The developed kinetics model based on cellular automata is reliable to describe the reduction process of pellets made by iron ores and reduced through a gas atmosphere featured by different concentrations of H_2 and CO; 2) The kinetics of reduction has been estimated correctly in the condition of static atmosphere as well as in the case of shaft furnace featured by counterflow between descending pellets and arising reducing gas; 3) A key point for the achievement of reliable estimation is the application of an update of concentration of reducing agent as a function of metallization, because the removal of oxygen improves the transport of reducing agent inside the pellets to be reduced; and 4) The computation time of the tested approach is compatible with in-line control of the system.

Acknowledgements

Conflict of Interest

The authors declare no conflict of interest.

Data Availability Statement

The data that support the findings of this study are available from the corresponding author upon reasonable request.

Keywords

[1] C. Mapelli, G. Dall'Osto, D. Mombelli, S. Barella, A. Gruttadauria, *Steel Res. Int.* **2022**, *93*, 2100631.
[2] D. Spreitzer, J. Schenk, *Steel Res. Int.* **2019**, *90*, 1900108.
[3] J. Tang, M. Chu, F. Li, C. Feng, Z. Liu, Y. Zhou, J. Tang, M. Chu, F. Li, C. Feng, Z. Liu, Y. Zhou, *Int. J. Miner. Metall. Mater.* **2020**, *27*, 713.
[4] J. Kim, B. K. Sovacool, M. Bazilian, S. Griffiths, J. Lee, M. Yang, J. Lee, *Energy Res. Soc. Sci.* **2022**, *89*, 102565.
[5] Z. Fan, S. J. Friedmann, *Joule* **2021**, *5*, 829.
[6] L. Holappa, *Metals* **2020**, *10*, 1117.
[7] B. Alamsari, S. Torii, A. Trianto, Y. Bindar, *Int. Scholarly Res. Network ISRN Mech. Eng.* **2011**, *2011*, 12.
[8] J. A. de Castro, E. P. Rocha, E. M. de Oliveira, M. F. Campos, A. S. Francsco, *Rev. Escola de Minas* **2018**, *71*, 81.
[9] D. Shiffman, S. Fry, Z. Marsh, in *Cellular Automata* (Ed: S. Fry), self-published by D. Shiffman, Mountain View **2012**, p. 498.
[10] A. Kireeva, K. K. Sabelfeld, S. Kireev, in *Parallel Computing Technologies* (Ed: V. Malyshkin), Springer International Publishing, Cham **2019**, https://doi.org/10.1007/978-3-030-25636-4_27.
[11] V. K. Vanag, *Phys. Usp.* **1999**, *42*, 413.
[12] R. M. D'Souza, N. H. Margolus, M. A. Smith, *J. Stat. Phys.* **2002**, *107*, 401.
[13] J. He, K. Li, J. Zhang, A. N. Conejo, *Metals* **2023**, *13*, 464.
[14] P. Metolina, T. R. Ribeiro, R. Guardani, *Int. J. Miner. Metall. Mater.* **2022**, *29*, 1908.
[15] K. Zygourakis, P. A. Markenscoff, *Biomaterials* **1996**, *17*, 125.
[16] N. Bertrand, G. Leclair, P. Hildgen, *Int. J. Pharm.* **2007**, *343*, 196.
[17] H. Laaksonen, J. Hirvonen, T. Laaksonen, *Int. J. Pharm.* **2009**, *380*, 25.
[18] L. B. Kier, C.-K. Cheng, H. T. Karnes, *Biomed. Chromatogr.* **2000**, *14*, 530.
[19] P. Córdoba-Torres, R. P. Nogueira, L. De Miranda, L. Brenig, J. Wallenborn, V. Fairén, *Electrochim. Acta* **2001**, *46*, 2975.
[20] O. Than, S. Büttgenbach, *Sens. Actuators, A Phys.* **1994**, *45*, 85.
[21] M. Tarabkhah, B. Khoshandam, *Transp. Porous Media* **2019**, *128*, 553.
[22] O. Bandman, *J. Supercomput.* **2011**, *57*, 121.
[23] C. Gu, C. D. Ridgeway, E. Cinkilic, Y. Lu, A. A. Luo, *J. Mater. Sci. Technol.* **2020**, *49*, 91.
[24] C. Pan, M. Hilpert, C. T. Miller, *Water Resour. Res.* **2004**, *40*, https://doi.org/10.1029/2003WR002120.
[25] S. Luo, M. Zhu, S. Louhenkilpi, *ISIJ Int.* **2012**, *52*, 823.
[26] Y. J. Lan, D. Z. Li, Y. Y. Li, *Acta Mater.* **2004**, *52*, 1721.
[27] W. Wang, C. Ji, S. Luo, M. Zhu, *Metall. Mater. Trans. B* **2018**, *49*, 200.
[28] M. Yamazaki, Y. Natsume, H. Harada, K. Ohsasa, *ISIJ Int.* **2006**, *46*, 903.
[29] H. Monshat, S. Serajzadeh, *Ironmaking Steelmaking* **2019**, *46*, 513.
[30] F. Chen, K. Qi, Z. Cui, X. Lai, *Comput. Mater. Sci.* **2014**, *83*, 331.
[31] D. Raabe, L. Hantcherli, *Comput. Mater. Sci.* **2005**, *34*, 299.
[32] B. J. Yang, L. Chuzhoy, M. L. Johnson, *Comput. Mater. Sci.* **2007**, *41*, 186.
[33] C. Zheng, N. Xiao, D. Li, Y. Li, *Comput. Mater. Sci.* **2008**, *44*, 507.
[34] C. Zheng, D. Raabe, *Acta Mater.* **2013**, *61*, 5504.
[35] A. D. Boccardo, P. M. Dardati, L. A. Godoy, *Mater. Sci. Technol.* **2018**, *34*, 1710.
[36] R. Zhou, X. Feng, C. Zheng, Q. Huang, Y. Li, Y. Yang, *Metals* **2023**, *13*, 368.
[37] H. Chen, Y. Chen, J. Zhang, *Prog. Nucl. Energy* **2008**, *50*, 587.
[38] X. Guo, J. Kang, J. Zhu, *J. Mater. Civil Eng.* **2018**, *30*, https://doi.org/10.1061/(ASCE)MT.1943-5533.0002502.
[39] K. He, Z. Zheng, Z. Chen, *Int. J. Hydrogen Energy* **2022**, *47*, 8118.
[40] K. He, Z. Zheng, Z. Chen, *Chem. Eng. Sci.* **2023**, *279*, 118947.
[41] Y. Korobeinikov, A. Meshram, C. Harris, O. Kovtun, J. Govro, R. J. O'Malley, O. Volkova, S. Sridhar, *Steel Res. Int.* **2023**, *94*, 2300066.
[42] A. Bonalde, A. Henriquez, M. Manrique, *ISIJ Int.* **2005**, *45*, 1255.
[43] H. Zuo, C. Wang, J. Dong, K. Jiao, R. Xu, *Int. J. Miner. Metall. Mater.* **2015**, *22*, 688.

[44] M. Kazemi, M. S. Pour, D. Sichen, *Metall. Mater. Trans. B* **2017**, *48*, 1114.

[45] J. Crank, *The Mathematics of Diffusion*, Oxford University Press, Oxford **1979**.

[46] L. S. Darken, *Trans. Aime* **1948**, *175*, 184.

[47] W. Pies, *Berichte der Bunsengesellschaft für physikalische Chemie* **1975**, *79*, 109.

[48] A. Agrawal, D. J. Gavel, M. B. Shaik, S. Dwarapudi, I. Paul, *J. Inst. Eng. Ser. D* **2021**, *102*, 87.

[49] H. bin Zuo, C. Wang, J. ji Dong, K. xin Jiao, R. sheng Xu, *Int. J. Miner. Metall. Mater.* **2015**, *22*, 688.

[50] M. Fanfoni, M. Tomellini, *Il Nuovo Cimento D* **1998**, *20*, 1171.

[51] D. R. Parisi, M. A. Laborde, *Chem. Eng. J.* **2004**, *104*, 35.